

utility inasmuch as CoFe_3S_4 clusters related to **13** are accessible using Co(I) reactants.²²

(2) The cluster products **9**, **10**, and **12** of (1) have cubane-type $[\text{NiFe}_3\text{Q}_4]^{1+}$ cores that differ only slightly in bond distances and volumes from the more familiar $[\text{Fe}_4\text{S}_4]^{2+,1+}$ clusters. One consequence of structural near-identity is the isomorphism and virtual inseparability of salts of $[\text{Fe}_4\text{Q}_4\text{L}_4]^{2-}$ and $[\text{MFe}_3\text{Q}_4\text{L}_4]^{2-}$ with the same cation (e.g., **6/11**). Consequently, reactions that afford heterometal subsite differentiation present an advantage if both MFe_3Q_4 and Fe_4Q_4 clusters are formed in the same system.

(3) Collective structural, magnetic, ^1H NMR, and Mössbauer²⁰ results support the fragment formulation $[\text{Fe}_3\text{Q}_4]^{1-}$ ($S = 5/2$) and Ni^{2+} ($S = 1$) as the zeroth-order description of charge distribution and antiparallel spin coupling between fragments as the origin of the $S = 3/2$ ground state. This mode of spin coupling results in oppositely signed isotropic (contact) shifts of identical ligands at iron and nickel subsites.

(4) Subsite-differentiated cluster **9** undergoes a variety of regiospecific substitution reactions to afford species with ligands such as phosphines, cyanide, and isonitrile at the nickel subsite. Detection of these reactions, which are sometimes accompanied by the formation of Fe_4S_4 cluster **4** as a byproduct, is facilitated by the large isotropic shifts afforded by the $S = 3/2$ ground state.

(5) The protein-bound NiFe_3S_4 species of *P. furiosus* Fd and synthetic $[\text{NiFe}_3\text{S}_4]^{1+}$ clusters (represented by **9**) have similar EPR spectra and the same ground state and thus are isoelectronic. It is entirely probable that the former has the cubane-type structure with a tightly bound nickel atom, as demonstrated for the synthetic clusters.

Seven heterometal cubane-type MFe_3S_4 clusters ($\text{M} = \text{V}, \text{Nb}, \text{Mo}, \text{W}, \text{Re}, \text{Co}, \text{Ni}$) have now been synthesized, some in several

different oxidation states.¹⁹ It appears that only lack of experimental ingenuity or of cluster stability will prevent incorporation of practically all metals into these clusters. Given the prevalence of Fe_4S_4 clusters, and detection of an increasing number of cuboidal Fe_3S_4 clusters, in many proteins and enzymes, a possible biological role for MFe_3S_4 species must be actively entertained. Our initial investigation of this matter with respect to one nickel-containing carbon monoxide dehydrogenase, by X-ray absorption spectroscopy, has shown that the NiFe_3S_4 cubane cluster is absent.⁶⁰ We are continuing our studies of MFe_3Q_4 clusters and their possible biological relevance. A forthcoming report will provide additional examples of reductive rearrangement reactions for the synthesis of these clusters.

Acknowledgment. This research was supported by NIH Grant GM 28856. X-ray equipment was obtained through NIH Grant 1 S10 RR 02247. We thank Russell Larsen for experimental assistance. EPR analysis software was furnished by the Illinois EPR Research Center, NIH Division of Research Resources Grant RR 01811.

Supplementary Material Available: Crystallographic data for the three compounds in Table I, including tables of intensity collections, atom and thermal parameters, bond distances and angles, and calculated hydrogen atom positions (21 pages); listings of calculated and observed structure factors (75 pages). Ordering information is given on any current masthead page.

(60) Tan, G. O.; Ensign, S. A.; Ciurli, S.; Scott, M. J.; Hedman, B.; Holm, R. H.; Ludden, P. W.; Korszun, Z. R.; Stephens, P. J.; Hodgson, K. O. *Proc. Natl. Acad. Sci. U.S.A.*, in press.

Transition-State Structural Variation in a Model for Carbonyl Reduction by Lactate Dehydrogenase: Computational Validation of Empirical Predictions Based upon Albery–More O’Ferrall–Jencks Diagrams

John Wilkie and Ian H. Williams*

Contribution from the School of Chemistry, University of Bath, Bath BA2 7AY, UK.
Received July 29, 1991

Abstract: The transition-state (TS) structure for reduction of formaldehyde by dihydropyridine (hydride donor) and imidazolium (proton donor) has been located and characterized by use of the AM1 semiempirical MO method. The hydride-transfer (HT) and proton-transfer (PT) components of this concerted reaction are kinetically coupled but dynamically uncoupled. Increasing the basicity of the imidazole moiety, by means of a suitably placed dipole of variable magnitude, leads to essentially no change in the degree of PT in the TS but to a substantial increase in the degree of HT. This computational result validates the prediction made on the basis of an Albery–More O’Ferrall–Jencks diagram. Correspondingly, the primary kinetic isotope effect (KIE) calculated for replacement of the transferring proton by a deuteron shows little change, but there is a significant increase in the magnitude of the calculated primary KIE for replacement of the transferring protide by a deuteride as the TS structure changes with increasing basicity of the imidazole moiety. This accords with the conventional view of the relationship between TS structure and the magnitude of primary KIEs.

The key to understanding of the fundamental processes of catalysis is the transition state (TS). It is of importance to know not only the nature of TS structure itself, but also the manner in which TS structure changes in response to changes within the reacting system and its environment, e.g., substituent and solvent effects, changes in acidity/basicity, or nucleophilicity/electrophilicity of reacting moieties. Physical organic chemists have developed empirical methods for rationalization of observed trends, as determined by experimental probes for TS structure including structure–reactivity correlations and kinetic isotope effects, and

have adopted these methods for predictive purposes.^{1,2} Of particular popular use has been the empirical construct known as the

(1) Thornton, E. K.; Thornton, E. R. In *Transition States of Biochemical Processes*; Gandour, R. D., Schowen, R. L., Eds.; Plenum: New York, 1978; pp 3–76.

(2) Jencks, W. P. *Chem. Rev.* **1985**, *85*, 511–527.

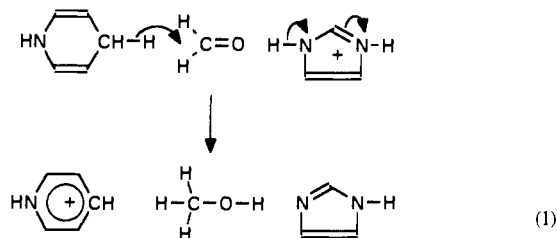
(3) Albery, W. J. *Prog. React. Kinet.* **1967**, *4*, 353–398.

(4) More O’Ferrall, R. A. *J. Chem. Soc. B* **1970**, 274–277.

(5) Jencks, W. P. *Chem. Rev.* **1972**, *72*, 705–718.

(6) Bruce, T. C. *Annu. Rev. Biochem.* **1976**, *45*, 331–373.

Scheme I



Albery³-More O'Ferrall⁴-Jencks⁵ (AMJ) diagram; this is a two-dimensional "map of alternative routes"⁶ with an implied third dimension of energy assumed to have the form of a saddle, thus representing the TS region of a potential energy surface for a reacting system. A change in, say, the acidity of a catalytic proton-donor group causes changes in the relative energies of one or more corners or edges of the diagram; the consequences for TS structure are deduced by consideration of the resultant of effects parallel and perpendicular to the reaction coordinate (see below). We now report the results of a computational study of variation in TS structure which confirms the validity of the empirical procedure for prediction of TS structural change using an AMJ diagram, and which also accords with the conventional view of the relationship between TS structure and the magnitude of a primary deuterium kinetic isotope effect (KIE).

Site-directed mutagenesis has afforded mutants of the enzyme lactate dehydrogenase (LDH) in which individual active-site residues have been substituted, and a wealth of kinetic, thermodynamic, and structural data now exists⁷ which has led to mechanistic hypotheses concerning the catalytic roles of several amino-acid side-chain groups; these now invite complementary investigation by computational modelling methods. As part of a larger program of modelling studies, we have performed quantum-chemical calculations, using the AM1 semiempirical molecular-orbital method,⁸ upon the uncatalyzed model reaction 1 (Scheme I) whose essential components are a hydride donor (dihydropyridine), HPyH, a carbonyl substrate (formaldehyde), and a proton donor (imidazolium cation, HIm⁺). Related theoretical studies by other groups have focused solely upon the hydride-transfer aspect.⁹⁻¹¹

LDH enzymes differ from alcohol dehydrogenases in that (among other things) the oxygen atom of the carbonyl group undergoing reduction is not coordinated to a zinc atom serving as a Lewis acid. A question of interest concerning the mechanism of LDH is this: do the hydride-transfer (HT) and proton-transfer (PT, although more properly hydron-transfer) components of the reduction occur concertedly or sequentially? The subject of the present paper, however, is not a theoretical simulation of the enzymic mechanism (which would obviously require consideration of the protein) but a theoretical investigation of TS structural variation in a gas-phase model (Scheme I) for the intrinsic reaction catalyzed by LDH; the model resembles the prototype in so far as it comprises both HT and PT components, but in other regards it is a very different process. What bearing the present results may have (if any) upon understanding the mechanism of the enzymic reaction will be deferred for discussion in a future paper devoted to theoretical modelling of aspects of catalysis by LDH.¹²

Methods

The MOPAC Version 6.0 program⁸ was used for semiempirical molecular-orbital calculations employing the AM1 Hamiltonian.¹³ Full geometry optimization (75 internal degrees of freedom) was performed

(7) Clarke, A. R.; Atkinson, T.; Holbrook, J. J. *Trends Biochem. Sci.* **1989**, *14*, 101-105, 145-148.

(8) Stewart, J. J. P. MOPAC 6.0: *QCPE Bull.* **1990**, *10*, 86-87.

(9) Wu, Y.-D.; Houk, K. N. *J. Am. Chem. Soc.* **1987**, *109*, 2226-2227.

(10) Krechl, J.; Kuthan, J. *J. Mol. Struct., THEOCHEM* **1988**, *170*, 239-244.

(11) Tapia, O.; Cardenas, R.; Andres, J.; Colonna-Cesari, F. *J. Am. Chem. Soc.* **1988**, *110*, 4046-4047.

(12) Clarke, A. R.; Osguthorpe, D. J.; Wilkie, J.; Williams, I. H. Manuscript in preparation.

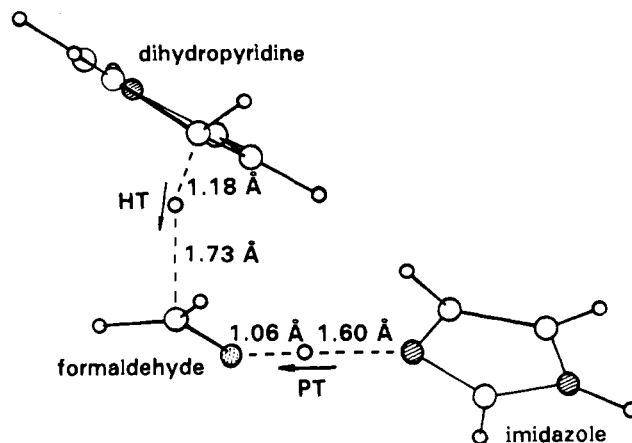
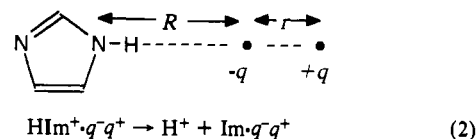


Figure 1. Fully optimized AM1 transition structure for the model reaction shown in Scheme I.

upon the reacting system, with Baker's eigenvector-following (EF) algorithm¹⁴ being used successfully (after some considerable effort) to locate a true first-order saddle point. The basicity of imidazole in the model reaction was altered by placing a dipole of variable magnitude behind the distal nitrogen atom of the heterocycle (Scheme II), in the same way as described previously to mimic pyridines of varying basicity.¹⁵ The dipole consisted of a pair of oppositely charged MOPAC "sparkles" (unit charges $q = |1|$) at the centers of spherical repulsive potentials. The negative sparkle was placed at a fixed distance of $R = 5$ Å from the NH nitrogen atom; by adjustment of the distance r to the positive sparkle (in the range 2-10 Å), the basicity of the imidazole could be modified. Gas-phase proton affinities (PAs) were calculated as heats of reaction (eq 2), where q^+q^- indicates a pair of sparkles whose dipole moment and

Scheme II



location were the same in reactant and product species. The experimental heat of formation of H⁺ was used in place of the AM1 value, in line with previous practice.¹⁶

Results and Discussion

Figure 1 shows the fully optimized TS structure for reaction 1, for which the residual components of the gradient are satisfactorily close to zero and which possesses a single imaginary vibrational frequency. Intrinsic reaction-coordinate calculations, following the gradient vector away from this saddle point, led only to reactant and product complexes for the model reaction. No evidence has been found for any other local minima on the AM1 energy hypersurface. In particular, no energy minima have been located corresponding to structures containing either the CH₃O⁻ or CH₂OH⁺ moieties, which would be part of the intermediate complexes occurring in stepwise mechanisms where HT precedes PT or vice versa. The structures and energies of the reactant and product complexes are dominated by electrostatic interactions peculiar to the model (and perhaps to the AM1 method) which are not germane to the present discussion of TS structural variation. The detailed values of geometrical parameters in the TS are likely to be specific to the calculational method, and no purpose is served by presenting any more than just those bond lengths (shown in Figure 1) of particular interest, which determine the extent of HT and of PT.

(13) Dewar, M. J. S.; Zoebisch, E. G.; Healy, E. F.; Stewart, J. J. P. *J. Am. Chem. Soc.* **1985**, *107*, 3902-909.

(14) Baker, J. *J. Comput. Chem.* **1986**, *7*, 385-395.

(15) Hammond, R. B.; Williams, I. H. *J. Chem. Soc., Perkin Trans. 2* **1989**, 59-66.

(16) Jorgensen, W. L. *J. Am. Chem. Soc.* **1978**, *100*, 1049, 1057. Olivella, S.; Urpi, F.; Vilarrasa, J. *J. Comput. Chem.* **1984**, *5*, 230-236. Dewar, M. J. S.; Dieter, K. M. *J. Am. Chem. Soc.* **1986**, *108*, 8075.

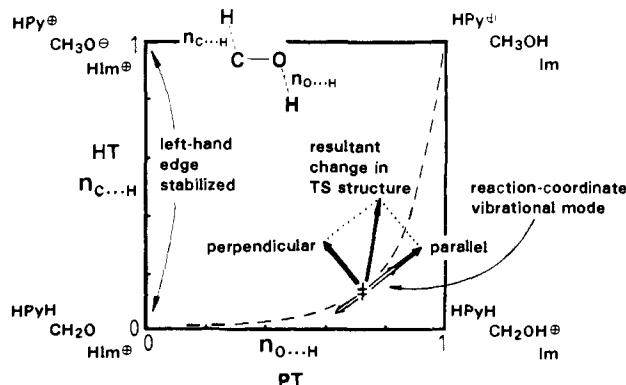


Figure 2. Albery-More O'Ferrall-Jencks diagram for the hydride-transfer and proton-transfer components of the model reaction, showing the location of the transition structure and illustrating the prediction of change in transition-state structure resulting from an increase in the basicity of the imidazole moiety.

The HT and PT components occur in roughly perpendicular planes. HT follows a Burgi-Dunitz¹⁷ approach of the nucleophile to the carbonyl π -system, and PT takes place along a preexisting hydrogen bond between the proton donor and an in-plane sp^2 lone pair on the carbonyl oxygen. This accords with expectation for the reverse reaction (dehydrogenation) based upon stereoelectronic considerations:¹⁸ departure of hydride as a leaving group from the alcohol is facilitated by an antiperiplanar lone pair in preference to an antiperiplanar OH bond (cf. ref 19). The reaction-coordinate vibrational mode in the TS for this concerted reaction (arrows on Figure 1, imaginary frequency $\nu^* = 287i \text{ cm}^{-1}$) comprises motions of both the hydride and the proton in the expected directions; the HT and PT components are thus kinetically coupled.²⁰ Geometrically, however, HT from HPyH has progressed to only a small degree in the TS, whereas PT from HIm⁺ is very advanced; in this sense HT and PT are dynamically uncoupled.²⁰ Figure 2 shows the position of the TS on an AMJ diagram whose axes are the Pauling bond orders²¹ of the C...H and O...H bonds being made to formaldehyde; the TS for the concerted reaction lies fairly close to the intermediate for a stepwise, specific acid-catalyzed reaction.

The residue aspartate-168 of LDH stabilizes the protonated form of histidine-195 in the ternary complex of the enzyme with cofactor NADH and substrate,²² and in various mutant enzymes the effective basicity of the imidazole group is modified. It is of interest to enquire how the TS structure for the model reaction 1 varies as the basicity of the imidazole moiety is raised. This change stabilizes HIm⁺ and so lowers the energy of the whole left-hand side of the AMJ diagram (Figure 2). The Hammond (parallel) effect of this change in exothermicity along the reaction coordinate is to shift the TS toward the top-right corner, and the anti-Hammond (perpendicular) effect is to shift the TS toward the top-left corner, since the energy of the unfavorable (HPy⁺ CH₃O⁻ HIm⁺) intermediate is reduced. The resultant of these component shifts leads to the prediction that increasing the basicity of imidazole should cause a significant increase in the degree of HT in the TS with very little change in the degree of PT.

The basicity of imidazole in the model reaction was altered by placing a dipole of variable magnitude behind the distal nitrogen atom of the heterocycle, in a position similar to that of aspartate-168 relative to histidine-195 in LDH. The TS structure was

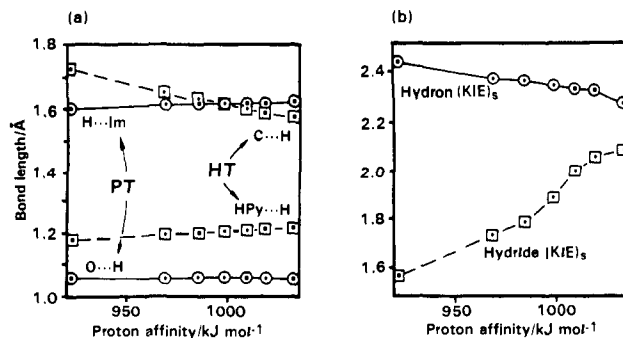


Figure 3. (a) Transition-state bond lengths and (b) semiclassical primary deuterium kinetic isotope effects for the hydride-transfer and proton-transfer components of the model reaction plotted against the proton affinity of the imidazole moiety.

reoptimized for each value of the dipole, corresponding to a different value of the proton affinity (PA) of the imidazole moiety. Figure 3a shows (solid lines) the O...H and H...Im bond lengths, involving the transferring proton, as a function of PA(Im); there is essentially no change in these distances as the PA increases from that of imidazole itself (922 kJ mol⁻¹ in AM1) up to 1035 kJ mol⁻¹. The dashed lines in Figure 3a show the HPy...H distance increasing slightly, and the C...H distance decreasing substantially, as PA(Im) rises; these bond-length changes involving the transferring hydride reflect a significant increase in the degree of HT with increasing basicity of the proton donor. These computational results verify the prediction based upon the AMJ diagram: increasing the basicity of the proton donor changes the TS structure in the direction of a more symmetrical HT component but with little or no change in the PT component.

It is often attempted to relate the magnitudes of primary hydrogen kinetic isotope effects (KIEs) in a family of reactions to the extent of hydrogen transfer in the TS.²³ Variation in TS structure from asymmetric and reactant-like, through symmetric, to asymmetric and product-like, is accompanied first by an increase and then by a decrease in the magnitude of the primary KIE as the transferring hydrogen (or deuterium) moves between the donor and acceptor species.²⁴ Semiclassical primary KIEs,²⁵ for substitution of the transferring proton by a deuterium ("hydron (KIE)_s") or of the transferring protide by a deuteride ("hydride (KIE)_s") in the family of model reactions 1, with imidazole groups of varying basicity, are plotted in Figure 3b against PA(Im). These are calculated from the AM1 geometries and vibrational frequencies, using molecular partition functions evaluated by means of the ideal-gas, rigid-rotor, and harmonic approximations. As the basicity of the imidazole increases, there is only a small downward drift in the isotope effect for the hydron transfer, but a substantial increase in the isotope effect for hydride transfer. This is in accord with there being essentially no change in the degree of PT, but a significant change in the degree of HT toward a more central and symmetrical TS.

Conclusions

It is gratifying to confirm that quantum-chemically calculated TS structural effects in this simple model reaction may be rationalized according to well-known principles and procedures of physical organic chemistry. The relevance of these results, and further modelling studies in progress in this laboratory, to the elucidation of the catalytic strategy employed by LDH will be discussed in detail in a forthcoming paper.

Acknowledgment. We thank the SERC, the Nuffield Foundation, and the Royal Society for financial support and A. R. Clarke and D. J. Osguthorpe for helpful discussions.

(17) Burgi, H. B.; Dunitz, J. D.; Lehn, J. M.; Wipff, G. *Tetrahedron* **1974**, *30*, 1563-1572.

(18) Deslongchamps, P. *Stereoelectronic Effects in Organic Chemistry*; Pergamon: Oxford, 1983.

(19) Pain, A. E.; Williams, I. H. *J. Chem. Soc., Chem. Commun.* **1988**, 1367-1368.

(20) Gandour, R. D.; Maggiora, G. M.; Schowen, R. L. *J. Am. Chem. Soc.* **1974**, *96*, 6967-6979.

(21) Bond order $n = \exp[(R_1 - R_n)/c]$, where R_1 and R_n are bond lengths for bonds of order unity and n , respectively, and the constant $c = 0.3$.

(22) Clarke, A. R.; Wilks, H. M.; Barstow, D. A.; Atkinson, T.; Chia, W. N.; Holbrook, J. J. *Biochemistry* **1988**, *27*, 1617-1622.

(23) Klinman, J. P. In *Transition States of Biochemical Processes*; Gandour, R. D., Schowen, R. L., Eds.; Plenum: New York, 1978; pp 165-200.

(24) More O'Ferrall, R. A. In *Proton-Transfer Reactions*; Caidin, E. F., Gold, V., Eds.; Chapman and Hall: London, 1975; pp 201-261.

(25) Melander, L.; Saunders, W. H. *Reaction Rates of Isotopic Molecules*; Wiley-Interscience: New York, 1980.